Technical note: Including non-evaporative fluxes enhances the accuracy of isotope-based soil evaporation estimates

Han Fu[1], Ming Gao[1], Huijie Li[2], Daniele Penna[3,4], Junming Liu[2], Bingcheng Si[2,5], and Wenxiu Zou[1]

[1] State Key Laboratory of Black Soils Conservation and Utilization, Northeast Institute of Geography and Agroecology, Chinese Academy of Sciences, Harbin 150081, China
[2] College of Hydraulic and Civil Engineering, Ludong University, Yantai 264025, China
[3] Department of Agriculture, Food, Environment and Forestry, University of Florence, Florence, Italy
[4] Forest Engineering Resources and Management Department, Oregon State University, Corvallis, USA
[5] Department of Soil Science, University of Saskatchewan, Saskatoon, SK S7N 5A8, Canada

Correspondence to: Wenxiu Zou (zouwenxiu@iga.ac.cn)

Abstract. Accurately estimating soil water evaporation is essential for quantifying terrestrial water and energy. Isotope-based methods are useful but often rely on steady-state (SS) soil water storage assumptions or non-steady-state (NSS) models that ignore non-evaporative fluxes (such as infiltration and transpiration), leading to mass balance errors. Here, we introduce a new framework, named ISONEVA (ISOtope based soil water evaporation estimation considers dynamic soil water storage and Non-EVAporative fluxes), adapted from lake evaporation models to account for both evaporative and non-evaporative fluxes in soils under dynamic soil water storage. Validation under virtual and field scenarios demonstrated that ISONEVA improved evaporation estimates by 54.1%-83.6% (virtual) and 54.5%-92.4% (field) compared to traditional SS and NSS models. Furthermore, ISONEVA estimated a plausible upper limit of the E/ET ratio (0.144), encompassing the observed value (0.126), whereas SS and NSS methods severely underestimated (0.035) or are unable to produce a limit under field validation. These results highlight the critical role of dynamic soil water storage and non-evaporative fluxes in isotope-based soil water evaporation estimates, offering a robust framework for long-term assessments and informing future coupled land surface modelling efforts.

1 Introduction

Evaporation is a fundamental component of the water and energy balance, consuming nearly one-quarter of incoming solar energy and playing a critical role in land-atmosphere interactions (Or et al., 2013; Trenberth et al., 2009). The long-term (decades) ratio of soil water evaporation (from here onward, simply termed as soil evaporation) to precipitation (E/P) provides key insights into ecohydrological processes, supports accurate water balance assessments, informs evapotranspiration (ET) partitioning, and improves hydrological model calibration (Benettin et al., 2021; Kool et al., 2014; Vereecken et al., 2016).

Stable isotopes in the water molecule (^{2}H and ^{18}O) have emerged as a powerful tool to directly estimate soil evaporation by tracing the enrichment in heavy isotopes ($\delta^{2}H$ and $\delta^{18}O$) in upper soil layers caused by evaporation-driven fractionation (Bailey et al., 2018; Rothfuss et al., 2020). Soil water evaporation and resulting isotope fractionation are highly transient due to dynamic solar radiation, wind speed and other meteorological factors. However, current isotope-based approaches rely on either steady-state (SS) or non-steady-state (NSS) frameworks. SS assumes constant soil water storage and isotopic composition over time, a condition rarely met in dynamic soil systems (Al-Oqaili et al., 2020; Xiang et al., 2021), yet its core assumption of constant water volume is only valid for large water bodies. NSS accounts for temporal variations in storage and isotopes but considers only evaporative fluxes (Gibson and Reid, 2010), neglecting subsurface flow (such as infiltration, root water uptake fluxes, and drainage), which can lead to biased estimates of evaporation (Mattei et al., 2020; Yidana et al., 2016). For example, some studies using NSS methods reported higher evaporation in forest sites compared to shrublands under similar meteorological conditions (Sprenger et al., 2017), contrasting the expectation that shrublands should exhibit greater soil evaporation due to more exposed soil and less canopy cover than forest (Benettin et al., 2021; Nicholls et al., 2023; Nicholls and Carey, 2021; Yu et al., 2022).

This discrepancy may reflect the influence of additional processes not fully accounted for in NSS methods, emphasizing the importance of explicitly representing non-evaporative fluxes, such as percolation and root water uptake, to ensure soil water and isotope mass balance when modelling soil evaporation. To address these limitations, we developed a new framework named ISONEVA (ISOtope based soil water evaporation estimation considers dynamic soil water storage and Non-EVAporative fluxes), extending the formulations originally derived for open water bodies (Gonfiantini, 1986). ISONEVA explicitly incorporates both evaporative and non-evaporative fluxes in the topsoil layer, offering a more realistic representation of soil processes and better soil water and isotope mass balance.

ISONEVA method is evaluated through a combination of virtual test and field lysimeter data, directly comparing it with SS and NSS approaches. By overcoming key theoretical and practical limitations of existing methods, ISONEVA is expected to be a promising tool for advancing soil evaporation assessments in diverse ecosystems and supports improved water resource management under climate changes. This study begins by outlining the theoretical basis of the ISONEVA framework and then evaluates its performance through a combination of virtual and field datasets. The objective is to explore the method's advantages, limitations, and its broader applicability in isotope-based hydrological studies.

2 Material and Methods

2.1 Method derivatives

A coordinate system is established with the zero-flux plane positioned at the soil surface, and the downward direction defined as positive. Within this framework, fluxes in the topsoil layer include precipitation (P), evaporation (E), and

percolation (Q). P and E have positive and negative directions, respectively; while the direction of Q depends on the balance between P and E: when E exceeds P over a given period, Q can be negative; conversely, when P exceeds E, Q is typically positive (Figure 1). Note that Q can be interpreted more broadly as the sum of all non-evaporative fluxes (do not result in significant isotopic fractionation) that leave the topsoil layer (positive sign), such as percolation and root water uptake (Fu et al., 2025).

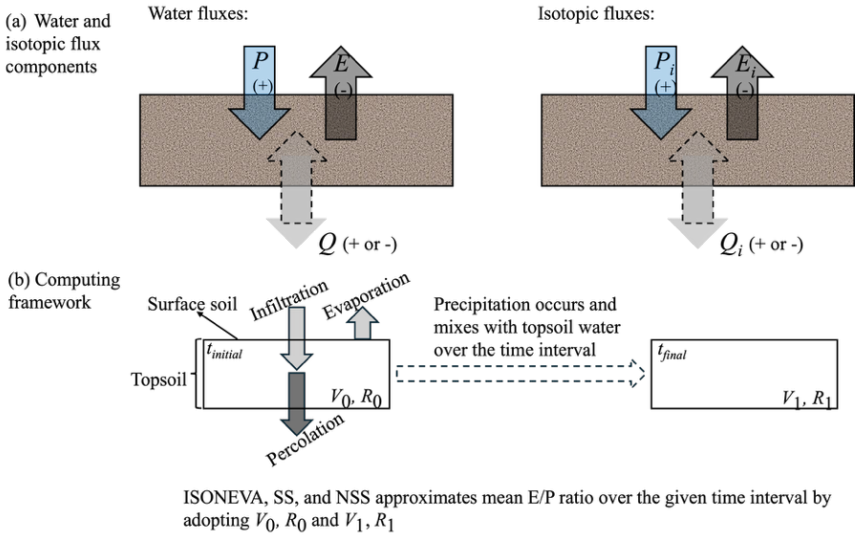

Figure 1. Conceptual illustration of the topsoil control volume and the water-isotope mass balance framework used in ISONEVA. (a) Schematic of water fluxes within the topsoil control volume, where *P*, *E*, and *Q* denote precipitation, evaporation, and percolation, respectively. Dashed arrows indicate that the direction of *Q* may reverse (upward or downward) depending on soil water potential gradients. (b) Conceptual diagram of the computational framework. ISONEVA, SS, and NSS use the initial ($t_{initial}$) and final (t_{final}) soil water content and isotopic composition (ratio, R) of the topsoil control volume to estimate the *E/P* ratio over the specified evaluation period.

Based on the defined system, the soil water and isotope mass balance can be written as:

$$\frac{\partial \theta}{\partial t} = -\frac{\partial q}{\partial z} \tag{1}$$

$$\frac{\partial (\theta R)}{\partial t} = -\frac{\partial q_i}{\partial z} \tag{2}$$

Note that for the convenience of calculation, isotopic ratio (R) is used in this study, instead of notation δ. The conversion between R and δ is:

$$\delta = \frac{R - R_{ref}}{R_{ref}} 1000 \tag{3}$$

where R_{ref} is the isotopic ratio reference value, 155.76×10^{-6} and $2{,}005.2 \times 10^{-6}$ for deuterium and oxygen-18, respectively.

Assuming the topsoil layer has a thickness of Δz and the variation of soil water and isotopic fluxes are uniform within the topsoil layer, then Eqs. (1) and (2) can be linearized as:

$$\frac{\partial \theta}{\partial t} = -\frac{\left(Q-(P+E)\right)}{\Delta z} \tag{4}$$

$$\frac{\partial (\theta R)}{\partial t} = -\frac{\left(Q_i-(P_i+E_i)\right)}{\Delta z} \tag{5}$$

with relationships between water and isotopic fluxes are:

$$\begin{cases} Q_i = QR \\ P_i = PR_P \\ E_i = ER_E \end{cases} \tag{6}$$

where R, R_P, and R_E are isotopic ratio of soil water in the topsoil layer, precipitation, and evaporation, respectively. We define the isotopic composition of infiltration to be equal to that of precipitation (Figure 1b). In addition, the isotopic composition of the outgoing percolation flux from the topsoil layer is assumed to be equal to the isotopic composition of the topsoil layer itself ($Q_i = QR$, Figure 1b). This treatment follows the well-established well-mixed control-volume assumption, whereby the measured bulk isotopic composition of the topsoil layer represents the integrated mixing of incoming precipitation with pre-existing soil water and thus defines the isotopic composition of water leaving the control volume. This assumption is widely adopted in isotope hydrology and solute transport modelling in porous media (e.g., Ads et al., 2025; Braud et al., 2005; Haverd and Cuntz, 2010; Zhou et al., 2021), as well as in isotope-based evaporation studies of open-water bodies (e.g., Gonfiantini, 1986).

Defining the soil water storage (V) of the topsoil layer is $\theta \Delta z$, then Eqs. (4) and (5) can be rewritten as:

$$\frac{\partial V}{\partial t} = P+E-Q \tag{7}$$

$$\frac{\partial (VR)}{\partial t} = PR_P+ER_E-QR \tag{8}$$

Combining Eqs. (7) and (8), the E/P ratio can be solved under different assumptions:

(1) SS method: Steady state evaporation characterized with constant soil water volume and isotopic ratio

When soil evaporation reaches a steady state, temporal variations in soil water storage and isotopic composition within the uppermost soil layer become negligible ($\frac{\partial V}{\partial t} = 0$ and $\frac{\partial (VR)}{\partial t} = 0$). Under these conditions, Eqs. (7) and (8) can be rewritten as:

$$P+E=Q \tag{9}$$

$$PR_P+ER_E=QR \tag{10}$$

Defining the ratio of evaporation to precipitation (E/P) as x and the ratio of Q to P as y, both can be solved analytically from Eqs. (9) and (10):

$$x=\frac{R\text{-}R_P}{R_E\text{-}R} \tag{11}$$

$$y=\frac{R_E\text{-}R_P}{R_E\text{-}R} \tag{12}$$

where R and R_P are measurable, R_E can be estimated using Craig-Gordon model:

$$R_E=\frac{E_i}{E} \tag{13}$$

where E and E_i are evaporative water and isotopic fluxes, respectively, based on the vapor concentration between soil surface and atmosphere:

$$E=\frac{cvsat\ RH_{soil}\ \text{-}cvsat\ RH_{atmos}}{\rho} \tag{14}$$

$$E_i=\frac{cvsat\ RH_{soil}\ \alpha\ R\text{-}cvsat\ RH_{atmos}\ R_{atmos}}{\alpha_k\ \rho} \tag{15}$$

where $cvsat$ is saturated vapor concentration, RH_{soil} and RH_{atmos} are soil and atmospheric relative humidity, respectively; R and R_{atmos} are isotopic ratio of soil and atmospheric water, α and α_k are equilibrium and kinetic fractionation factors (Fu et al., 2025). Note that the estimated value of x (Eq. 11) should be negative, as the negative sign indicates the direction of evaporation is opposite to that of precipitation (P).

Consequently, Eq. (13) can be rewritten by combining Eqs. (13), (14) and (15):

$$R_E=AR\text{-}B \tag{16}$$

with $A=\frac{RH_{soil}\ \alpha}{\alpha_k}$, $B=\frac{RH_{atmos}\ R_{atmos}}{\alpha_k}$.

(2) NSS method: Non-steady state characterized by dynamic soil water volume and isotopic ratio, but caused by evaporation only

Under this framework, Eqs. (7) and (8) can be simplified as:

$$\frac{\partial V}{\partial t}=E \tag{17}$$

$$\frac{\partial (VR)}{\partial t}=ER_E \tag{18}$$

Defining the ratio of final soil water storage (V) to the initial soil water storage (V_0) is f ($f=\frac{V}{V_0}$). R can be analytically derived from Eqs. (17) and (18) (Derivations can be referred to Appendix A):

$$R=\text{-}\frac{B}{1\text{-}A}+f^{\text{-}(1\text{-}A)}\left(R_0+\frac{B}{1\text{-}A}\right) \tag{19}$$

where R_0 is the initial soil water isotopic ratio; A and B are defined in Eq. (16). Note that Eq. (19) is generally written in the following form to estimate remaining water fraction of V_0 after evaporation:

$$f=\left(\frac{R+\frac{B}{1-A}}{R_0+\frac{B}{1-A}}\right)^{\frac{1}{1-A}} \tag{20}$$

Then, the evaporative loss fraction of the initial soil water volume (f_e) can be calculated as:

$$f_e=1-f=1-\left(\frac{R+\frac{B}{1-A}}{R_0+\frac{B}{1-A}}\right)^{\frac{1}{1-A}} \tag{21}$$

Consequently, the ratio of evaporation to precipitation, x, can be written as:

$$x=\frac{V_0 f_e}{P} \tag{22}$$

(3) ISONEVA: Non-steady state evaporation characterized with dynamic soil water storage and isotopic ratio resulted from evaporative and non-evaporative fluxes

When evaporative and non-evaporative fluxes in the topsoil layer are considered, R can be derived from Eqs. (7) and (8) without simplifications (see Appendix A for derivations):

$$R=\frac{R_P-Bx}{1-Ax+x}+f^{\frac{1-Ax+x}{1+x-y}}\left(R_0-\frac{R_P-Bx}{1-Ax+x}\right) \tag{23}$$

Solutions of x and y from Eq. (23) are introduced in virtual test section and all parameters in Eq. (23) are already defined.

2.2 Method evaluation

Virtual test

The virtual test scenario is adapted from a benchmark case, which is characterized by an unsaturated soil column evaporate under non-isothermal conditions and it has been employed in several hydrological model validation studies (Fu et al., 2025; Zhou et al., 2021). In this study, the boundary conditions of this benchmark are modified: (1) the upper boundary condition is changed from evaporation-only to include both evaporation and precipitation; (2) the lower boundary condition is switched from water supplementation to free drainage. Using the modified setup, soil water and isotope profiles within a 1-meter-deep soil column are simulated over a 100-day period using the MOIST model, whose capability to accurately simulate isotope transport in soil has been demonstrated by Fu et al. (2025).

Note that the MOIST model generates the isotopic composition for all fluxes such as evaporation and percolation from the simulated topsoil water, while rainfall isotopic composition is provided as a direct input. These data are then used to assess the accuracy of SS, NSS, and ISONEVA by comparing their estimated E/P ratios with the true values derived from MOIST-simulated evaporation and precipitation fluxes across various temporal and spatial scales. This virtual experiment serves as a controlled benchmark and it is designed to test our core hypothesis: by integrating both evaporative and non-evaporative fluxes, ISONEVA's more rigorous enforcement of mass conservation yields more accurate E/P estimates than the existing approaches.

Soil information

The simulated soil texture is Yolo light clay (Braud et al., 2005). The relationships between soil water content, pressure head, and unsaturated hydraulic conductivity for this soil type is described using the Brooks-Corey model (Brooks & Corey, 1964).

Initial and boundary conditions

The initial condition of soil water content is uniformly distributed with a value of 70% saturated soil water content, while the initial isotope profile ($\delta^{18}O$) is uniformly distributed with a value of 0‰. The air temperature and relative humidity are maintained at 40°C and 0.2, respectively, throughout the simulation (Figure 2). The potential evaporation rate is 2×10^{-7} m s^{-1}. Rainfall is assumed to occur every 5 days, with a flux of $\epsilon\times3\times10^{-7}$ m s^{-1} per event, where ϵ is a random number between 0 and 1. The isotopic signature ($\delta^{18}O$) of each rainfall event is randomly assigned within the range -50‰ to -10‰ using $-50+\epsilon\times40$ (‰), which is sufficient to encompass the natural variability of precipitation $\delta^{18}O$ observed across a wide range of climatic conditions (Nelson et al., 2021).The lower boundary condition is set as free drainage for both water and isotope transport, implying zero gradients in both soil water potential and soil water isotope compositions at the bottom.

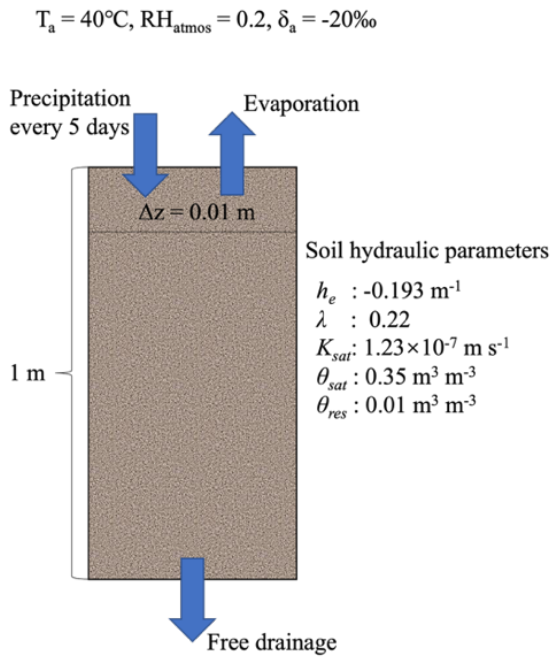

Figure 2. Description of the simulated soil column and boundary conditions used in MOIST. T_a, RH_{atmos}, and δ_a are atmospheric temperature, atmospheric relative humidity, and atmospheric isotopic compositions of oxygen-18; h_e, λ, k_{sat}, θ_{sat}, and θ_{res} are air entry value, pore size distribution parameter, saturated hydraulic conductivity, saturated soil water content, and residual soil water content; Δz denotes the spatial discretization step.

E/P ratio evaluation

MOIST outputs soil water and oxygen-18 profiles on a daily scale over a 100-day simulation period. Then, these simulated data are used in SS (Eq. 11), NSS (Eq. 19), and ISONEVA (Eq. 23) to back-calculate E/P ratio. Additionally, the true E/P ratio can be calculated directly from the simulated evaporation and precipitation fluxes provided by MOIST.

Various temporal intervals (from 5 to 100 days) and five spatial intervals (0.01, 0.05, 0.08, 0.1, and 0.2 m) are considered for E/P estimation. The selected time intervals ensure that at least one rainfall event occurs within each period. For a given evaluation interval, the initial and final soil water content and isotopic composition of the topsoil layer are obtained from the MOIST simulations and used as inputs to estimate the E/P ratio over that interval. For example, for a 5-day interval, soil water content and isotopic composition on Day 1 and Day 5 are used to estimate the E/P ratio for those five days.

The spatial intervals are selected to reflect typical soil water isotope sampling depths in field studies, where the thickness of the topsoil generally within 0.2 m (Dubbert et al., 2013; Shokri et al., 2008). Then, MOIST is applied to each of the spatial intervals for simulating soil water, isotope, flux profiles, which are used by SS, NSS, and ISONEVA to estimate E/P (Q/P) ratios reversely.

Note that due to the strong linear correlation between δ^2H and $\delta^{18}O$, particularly under the idealized conditions simulated by MOIST, they provide redundant rather than complementary information. As a result, they cannot be jointly used to independently constrain both x and y. Therefore, $\delta^{18}O$ is used as the representative tracer in this virtual test.

Since SS and NSS contain only one unknown, which can be solved directly using output data from MOIST. By contrast, ISONEVA involves two unknowns but only one equation, making it an underdetermined problem that lacks a unique analytical solution. Consequently, we rewrite Eq. (23) as the objective function:

$$F(x, y)=abs\left(\frac{R-\frac{R_P-Bx}{1-Ax+x}}{R_0-\frac{R_P-Bx}{1-Ax+x}}f^{\frac{1-Ax+x}{1+x-y}}\right) \tag{24}$$

To optimize Eq. (24), we employ a numerical approach that combines Genetic Algorithm (GA) optimization with Monte Carlo simulation. GA is a stochastic global optimization technique well-suited for exploring complex and non-convex solution spaces, but its random nature can lead to variability in the results. To improve reliability and capture the full range of plausible solutions, we embed the GA within a Monte Carlo framework: each group consists of 500 independent GA runs, and the process is repeated 100 times. The pseudo-posterior distributions of E/P (and Q/P) can be generated, and E/P (Q/P) estimates are reported in the form of mean ± standard deviation.

The bounds for variables x (E/P) and y (Q/P) in Eq. (24) are [−20, 0] and [−20, 1], respectively. The negative bound for x reflects the potential opposite direction of evaporation relative to precipitation, while the upper limit of 1 for y represents the scenario where all precipitation infiltrates downward as percolation or(and) root water uptake. A negative lower bound for y indicates the potential upward flux compensation from lower layers to topsoil layer under large evaporation situations.

Note that Eq. (24) contains an optimization trap: when x approaches 1/(A - 1), Eq. (24) approaches zero. This may cause the solver to converge to 1/(A - 1), even though this value is not necessarily the wanted one. To avoid this issue, we added a penalty term to Eq. (24):

$$F(x, y)=abs\left(\frac{R-\frac{R_P-Bx}{1-Ax+x}}{R_0-\frac{R_P-Bx}{1-Ax+x}}f^{\frac{1-Ax+x}{1+x-y}}\right)+\frac{p_s e^{\left(-\left(x-\frac{1}{A-1}\right)^2\right)}}{p_w} \tag{25}$$

where p_s and p_w represent the penalty strength (10) and penalty width (1×10^{-4}), respectively. This penalty term ensures that when x approaches 1/(A - 1), the penalty becomes stronger, while it remains negligible when x is far from 1/(A - 1), thereby preventing the optimizer from falling into the optimization trap.

Field test

Site description

The field experiment is conducted on continuously weighted soil lysimeters, situated at the École Polytechnique Fédérale de Lausanne (EPFL), in Switzerland (Nehemy et al., 2021). Lysimeters are exposed to atmospheric conditions and monitored for a period of 43 days after the application of an isotopically labelled irrigation event on the 16 May 2018, ending on the 29 June 2018. One bare lysimeter and one vegetated lysimeter are used to monitor evaporation and evapotranspiration, respectively.

Measured data

Within the vegetated lysimeter, soil water content is measured at four depths (0.25, 0.75, 1.25, and 1.75 m) using frequency domain reflectometry probes (FDR; 5TM Devices Inc., USA), while soil water isotopic compositions are sampled at five depths (0.1, 0.25, 0.5, 0.8, and 1.5 m) and analysed at the Watershed Hydrology Lab at the University of Saskatchewan. To harmonize the spatial scales of these two datasets, we define 0-0.25 m as the topsoil layer. Details about the experiment and sample processing can be referred to Nehemy et al., (2021).

Since evaporation measurements from the neighbour bare lysimeter are only available between 4 June and 29 June, thus, the field validation in this study is conducted in this period. Within this period, the daily evaporation rate (measured by the bare soil lysimeter) ranged from 0.97 to 2.27 mm day^{-1} (Figure 3). Three precipitation events (including artificial irrigation) took place on June 10, 14, and 26. The smallest daily input is 69.2 mm day^{-1} (on June 10), while the largest input is 193.5 mm day^{-1} (on June 26) (Figure 3). The input isotopic signals showed a gradual depletion as the precipitation amount increased (Figure 3).

Under this water input pattern, soil water content in the uppermost layer (0-0.25 m) shows a “rise-decline-rise” trend (Figure 3). Notably, unlike the strong correlation linear trend between hydrogen and oxygen stable isotopes in precipitation, the isotope signals in soil water did not exhibit a fully synchronized or linear pattern of change (Figure 3).

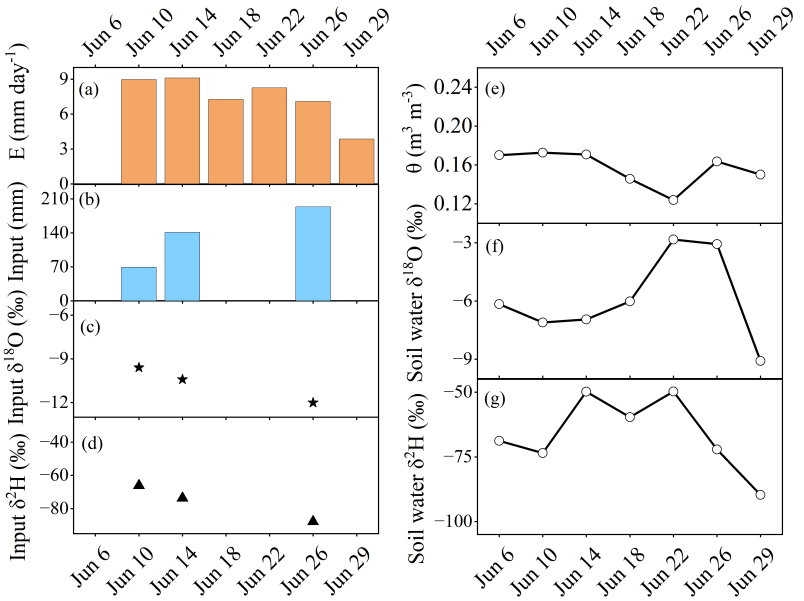

Figure 3. Measured evaporation (panel a), input water (precipitation + irrigation, panel b) and isotope signals (panels c and d), soil water contents (panel e) and isotopic signals (panels f and g) from June 6 to June 29. Note that June 6 is the initial date.

E/P estimation

Following the sampling frequency from Nehemy et al. (2021), several time intervals (4, 8, 12, 16, 20, and 24 days) are defined to estimate the E/P ratio for each period, starting from June 4. Meanwhile, actual E/P ratios are calculated using evaporation data from the bare lysimeter, serving as a benchmark for evaluating the performance of SS, NSS, and ISONEVA.

The potential daily evaporation (E_p) is conservatively assumed to range between 0.1 and 10 mm day^{-1}. Consequently, the lower and upper bounds of E/P are set based on the ratio of total E_p to precipitation during each time interval. To account for the effects of root water uptake and artificial irrigation, the bounds for y are set from 0 to 1. Hydrogen and oxygen stable isotopes are independently used in separate optimization runs, and their estimations are averaged as the final E/P (as well as Q/P) for each time interval (Sprenger et al., 2017).

The isotopic composition of infiltration is set equal to that of rainfall, which is a standard measurement during field campaigns and has been justified in Figure 1. For the non-evaporative flux, we assign the isotopic composition of the topsoil water. This is justified because (1) non-evaporative flux is expected to cause insignificant isotopic fractionation, and (2) the isotopic composition of topsoil water is directly measurable. Additionally, due to the absence of in situ measurements of atmospheric water vapor isotopes, we adopt reference values of δ^2H = -140‰ and $\delta^{18}O$ = -20‰ based on cold-trap measurements conducted in Vienna under comparable climatic and seasonal conditions (Kurita et al., 2012). Global water

vapor isotope studies indicate that central European stations exhibit strong spatial coherence in vapor isotopic composition, with $\delta^{18}O$ values typically clustering between -25‰ and -15‰ because of the dominant mid-latitude westerly circulation (Galewsky et al., 2016). Because the EPFL site in Lausanne is located within this same large-scale meteorological regime, its atmospheric vapor isotopic composition is expected to fall within this characteristic range. To adopt a conservative approach, we further evaluated the sensitivity of our results to vapor isotope uncertainty by testing a substantially wider range of values (-27‰ to -13‰ for $\delta^{18}O$ and -199‰ to -94‰ for $\delta^{2}H$; Kurita et al., 2012) in Appendix B. This range far exceeds the plausible climatological differences between Vienna and Lausanne. The resulting variation in estimated E/P ratios is modest, indicating that our conclusions are robust to uncertainties associated with the use of non-local vapor isotope data.

ET partition

When assuming the topsoil layer root water uptake flux dominates the non-evaporative flux Q, Q/P can be reasonably interpreted as T/P (the ratio of transpiration to precipitation):

$$\frac{Q}{P} \approx \frac{T}{P} \tag{26}$$

Consequently, E/ET can be estimated by:

$$\frac{E}{ET} = \frac{\frac{E}{P}}{\frac{E}{P} + \frac{Q}{P}} = \frac{x}{x+y} \tag{27}$$

Note that the derived E/ET from Eq. (27) represents an upper bound of the true E/ET ratio. This is because Q only accounts for transpiration originating from the uppermost soil layer (top 0.25 m in our field validations), whereas total transpiration (T) may also include contributions from deeper soil layers. When root water uptake occurs below the uppermost layer, or when percolation from the topsoil is non-negligible, $Q < T$, leading to an underestimate of total ET and, consequently, an overestimate of E/ET. This assumption is therefore used solely to construct a physically constrained upper limit on T/ET, representing the maximum plausible transpiration fraction consistent with water and isotope mass balance. It should not be interpreted as describing actual root water uptake patterns in specific ecosystems. Furthermore, under extremely arid conditions without rainfall input ($P = 0$), ISONEVA cannot estimate E/P and thus cannot be used for ET partitioning. Consequently, the upper-bound T/ET estimate is not intended for application in arid regions. Unless transpiration from deeper soil layers (below topsoil layer) and percolation fluxes are negligible, the E/ET values obtained using this approach should be interpreted as upper limits rather than exact estimates.

Method accuracy

In both the virtual and field validations, SS and NSS are applied using the same inputs, temporal resolution, and initial and final soil water and isotope profiles as the ISONEVA method. This ensures a fair comparison, removing the potential effects of data on the performance improvement of ISONEVA.

Accordingly, to quantify the accuracy of the average E/P value approximated by SS, NSS, and ISONEVA, we assess model performance using the mean absolute error (MAE):

$$MAE=abs(EP_{ei}- EP_{mi}) \quad (28)$$

where EP_{ei} and EP_{mi} are estimated and measured (or estimated from MOIST in virtual tests) E/P values; N is the total number of measurements; i is the i^{th} measurement.

3 Results

3.1 Comparison of estimated E/P and Q/P ratios between SS, NSS, and ISONEVA from virtual dataset.

Across all spatial and temporal intervals, SS often produces E/P estimates based on SS often deviate markedly from the true values, especially for thicker soil layers and larger time intervals (Figures 4a-4e). This bias arises from its inability to account for soil water storage dynamics (Eq. 11). While NSS considers soil water storage dynamic, it still systematically underestimates E/P (Figures 4a-4e) due to ignoring non-evaporative fluxes (infiltration) and resulted in poor soil water mass balance (Eq. 22).

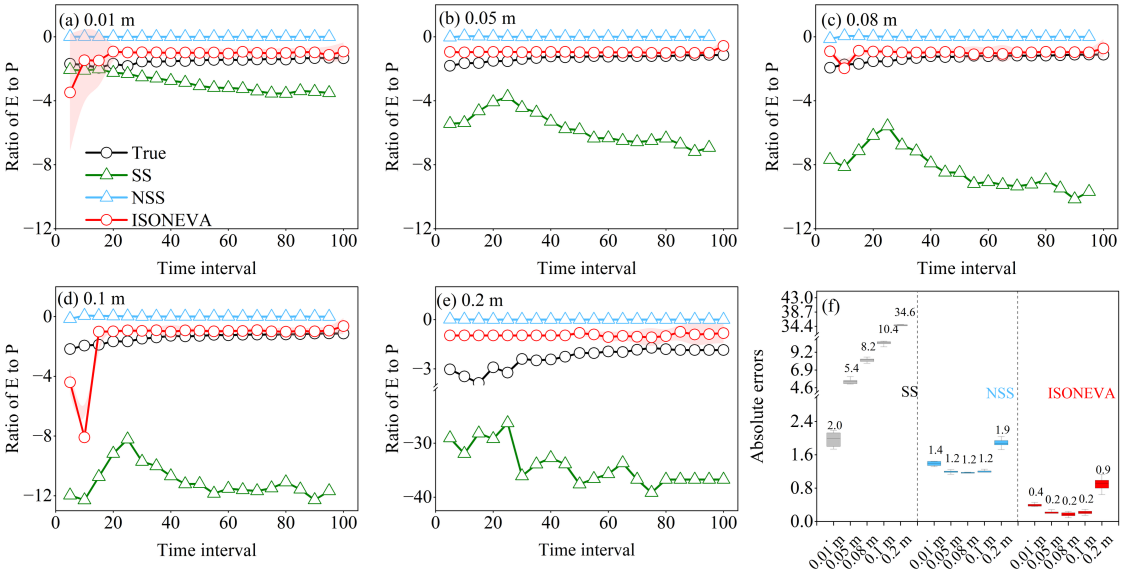

Figure 4. Comparison of estimated soil water evaporation to precipitation ratios (E/P) using the steady-state (SS), non-steady-state (NSS), and ISONEVA methods across varying topsoil layer thicknesses: (a) 0.01 m, (b) 0.05 m, (c) 0.08 m, (d) 0.1 m, and (e) 0.2 m, under various time intervals in x axis (from 5 to 100 days). Simulated ratios from MOIST are served as true values. Note that E/P estimates are negative because we defined a downward positive direction of fluxes. Additionally, absolute error of E/P estimates for each method and layer thickness are shown in panel f. Numbers above the box in panel f are mean absolute errors.

By contrast, ISONEVA provides the most accurate and stable E/P estimates across all scenarios. Its performance is particularly robust at medium to long time intervals (≥30 days). It is worth noting, however, that at very short intervals (5-10

days), ISONEVA may yield higher errors (particularly for fine layers) and occasionally exceeded those of the SS method (Figure 4a). This is because over short timescales, topsoil water storage varies little, making the steady-state assumption approximately valid and limiting the advantage of ISONEVA. As water storage variations grow with time (larger time intervals), ISONEVA becomes increasingly effective.

These differences are quantitatively summarized in Figure 4f. ISONEVA consistently yields the lowest MAE of E/P estimates, reducing error by over 80% on average compared to SS and NSS methods. Unlike SS, whose error increases monotonically with topsoil layer thickness, NSS and ISONEVA both show a U-shaped response: errors initially decrease with increasing topsoil layer thickness, reaching a minimum around 0.08 m, and then rise again. This U-shaped relationship arises likely because overly thin topsoil layers (e.g., 0.01 m) amplify sensitivity to isotopic fluctuations, leading to large errors. As thickness increases to 0.08 m, errors decrease due to improved signal stability without excessive smoothing. Beyond 0.08 m, further thickening (e.g., 0.2 m) dilutes isotopic gradients, reducing sensitivity and increasing errors again. Thus, 0.08 m topsoil layer thickness represents an optimal trade-off between resolution and robustness.

Figure 5 compares estimated Q/P ratios using the SS and ISONEVA methods against the true values (simulated by MOIST) across a range of topsoil layer thicknesses (0.01, 0.05, 0.08, 0.1, and 0.2 m) as a function of temporal intervals (5 to 100 days). NSS method is excluded from this comparison because it does not account for non-evaporative fluxes and thus cannot provide Q/P estimates.

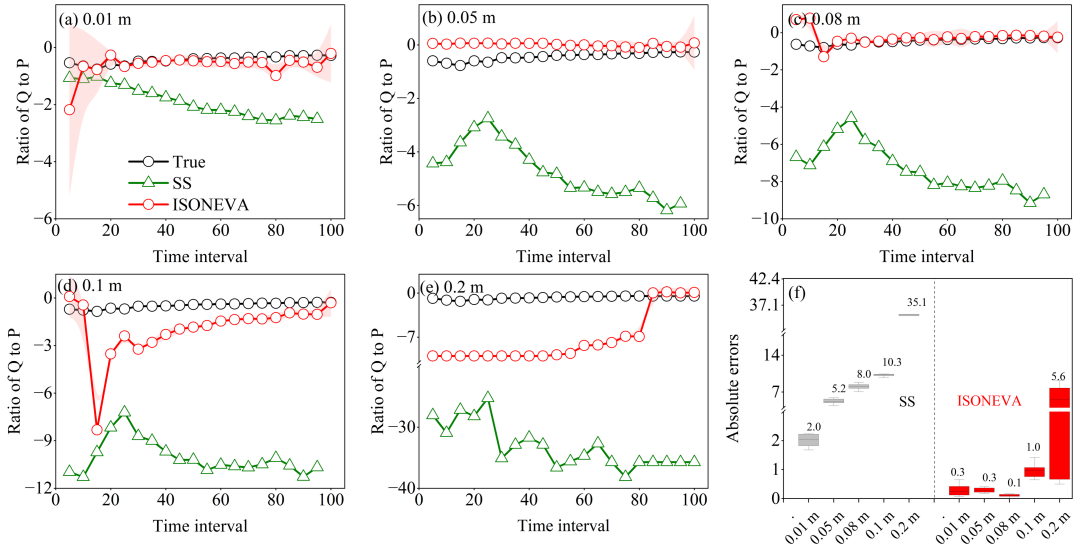

Figure 5. Estimated Q/P ratios using the steady-state (SS) and ISONEVA methods across different topsoil thicknesses: (a) 0.01 m, (b) 0.05 m, (c) 0.08 m, (d) 0.1 m, and (e) 0.2 m, under various time interval (from 5 to 100 days). Simulated Q/P values from MOIST are used as the reference ("True"). Panel f showed absolute errors of SS and ISONEVA methods across all scenarios. Numbers above the box in panel f are mean absolute errors.

The estimated Q/P values from SS often deviate significantly from true Q/P values, especially at larger topsoil thicknesses and longer time intervals (Figures 5a to 5e). By contrast, ISONEVA consistently produces more accurate Q/P estimates, particularly under 0.01, 0.05, and 0.08 m topsoil layer thickness. At these depths, ISONEVA closely tracks the true Q/P values across the full range of integration intervals, with only minor fluctuations under very short time intervals (e.g., <20 days). For thicker layers (0.1 and 0.2 m), however, ISONEVA initially exhibits large deviations, but accuracy improves markedly with increasing time intervals.

The errors of SS and ISONEVA are quantitatively illustrated in Figure 5f. The SS method exhibits a sharp increase in MAE with increasing topsoil thickness, from 2.0 at 0.01 m to 35.1 at 0.2 m. By contrast, ISONEVA substantially reduces errors across all scenarios, with values as low as 0.1-0.4. Note that the smallest error of Q/P from ISONEVA is observed from 0.08 m topsoil layer, consistently with the E/P results reported in Figure 1f. This convergence in both E/P and Q/P estimation performance supports that 0.08 m is the optimal topsoil thickness when applying ISONEVA for soil water evaporation estimates.

3.2 Field test

Field validation of the SS, NSS, and ISONEVA methods over a 23-day period (June 6-29) is shown in Figure 6, based on soil water and isotopic measurements from a vegetated lysimeter experiment under real-world conditions.

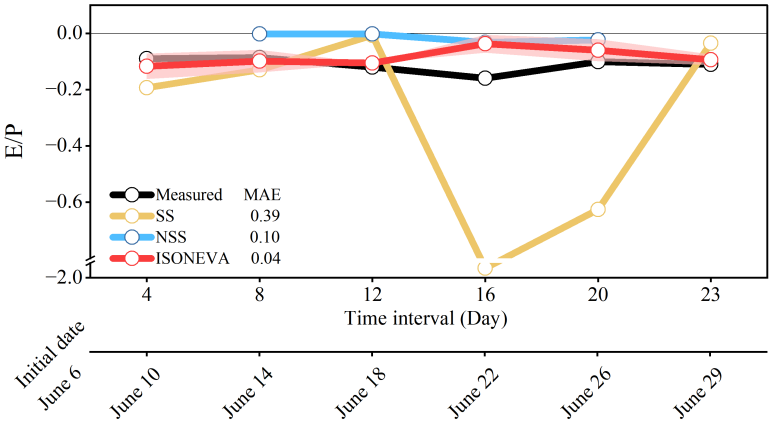

Figure 6. Estimated and measured E/P ratios from lysimeter data under different temporal intervals. The shaded pink area represents the uncertainty of ISONEVA estimates. The date is shown on the lower x-axis.

While SS estimates are acceptable at shorter intervals (e.g., 4 and 8 days), their accuracy rapidly dropped with longer intervals (Day 16 and 20), mirroring the trends in virtual simulations. However, the NSS method, which relaxes the steady soil water storage constraint, showed moderate improvements (MAE = 0.10) but still systematically underestimated E/P due to the failure of considering non-evaporative fluxes (e.g., infiltration). Also note that NSS does not converge for the first and last evaluation intervals because the method assumes that changes in soil water storage are driven solely by evaporation.

This assumption is violated when the observed soil water and isotope data reflect additional processes, such as infiltration or strong isotopic perturbations. The spiking experiment at the field site caused large shifts in topsoil isotopic composition that cannot be reconciled within the NSS framework, leading to failure in estimating E/P for these intervals (Figure 6).

By contrast, the ISONEVA method delivered the highest accuracy (MAE = 0.04), closely aligning with measured E/P values throughout the period. This confirms the importance of incorporating both evaporative and non-evaporative fluxes to estimate soil evaporation using field-measured isotope data.

Additionally, cumulative ET from the vegetated lysimeter was 351.25 mm, and cumulative E from the bare lysimeter was 44.25 mm, yielding an observed E/ET ratio of 0.126. Based on the total precipitation input (403.65 mm), ISONEVA estimated an E/P ratio of 0.09 ± 0.019, corresponding to an inferred E/ET ratio of 0.103 ± 0.019. This value slightly underestimates the observed ratio, which is consistent with expectations under vegetated conditions. When accounting for uncertainty associated with atmospheric vapor isotopic composition, quantified as a sensitivity-derived range of approximately ±0.015 in E/P based on Appendix B (Table B1), together with the intrinsic uncertainty of the ISONEVA model (±0.019), a conservative uncertainty envelope of ±0.024 is obtained for the inferred E/ET ratio (0.103±0.024). This range remains consistent with the observed E/ET ratio (0.126). By comparison, the SS and NSS methods yielded significantly lower E/ET values of 0.026 and 0.04, respectively, substantially underestimating soil water evaporation.

Even in the absence of direct ET measurements, ISONEVA provides a conservative upper bound estimate of E/ET as 0.144, which successfully encompassed the observed value (0.126). By contrast, the upper bound from SS is 0.035 and failed to do so. This further demonstrates the practical utility of ISONEVA in real-world applications, especially where direct ET partitioning is unavailable.

4 Discussion

4.1 ISONEVA improves solution space and avoids potential issues from identifying initial values

ISONEVA is more accurate than SS and NSS methods because it explicitly integrates temporal changes in soil water content and isotopic composition, as well as both evaporative and non-evaporative fluxes, which are ignored by SS and NSS. By introducing non-evaporative fluxes (Q), ISONEVA expands the solution space, allowing estimates to better approach the global optimum and reducing biases caused by oversimplified assumptions. As shown in Figure 7, including Q broadens the region of feasible solutions with lower objective function values (highlighted in yellow), thus enhancing the robustness and accuracy of E/P estimates.

The contour map further illustrates why Q/P estimates from ISONEVA are more sensitive than those of E/P, as reflected in the MAE variations (Figures 4f and 5f). This is primarily because the gradient of the objective function in ISONEVA (Eq. 25) is steeper along the Q/P axis than along the E/P axis within the feasible range (Figure 7). Future studies could incorporate additional constraints, such as energy balance, to further narrow the solution space for Q/P and enhance the stability and reliability of model estimates. Despite the expanded solution space, the optimization problem in ISONEVA remains well constrained. Although a Genetic Algorithm (GA) is used as a general-purpose solver, repeated optimization runs consistently converged to the same solution with small numerical variance, which is much smaller than the methodological differences at monthly timescales (Figures 4 and 5). This confirms that the improved performance of ISONEVA arises from its more complete physical formulation rather than from numerical artifacts associated with the optimization procedure.

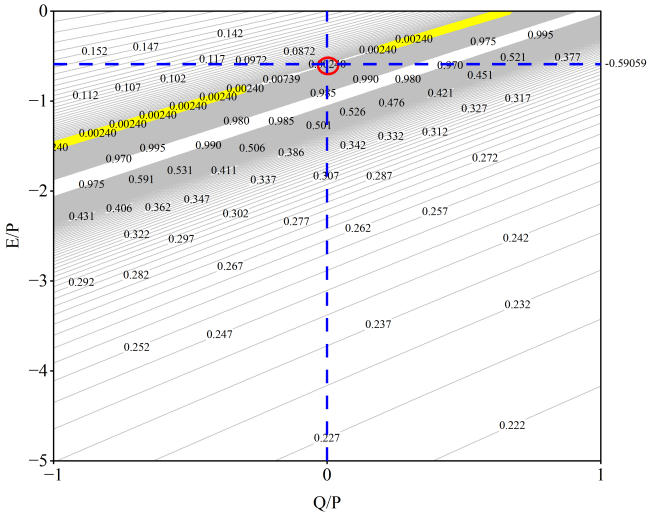

Figure 7. Contour map of Q/P vs. E/P fluxes based on the ISONEVA method generated using MOIST-simulated soil water content and isotope data during the first 5-day interval with a 0.01 m spatial resolution. The red circle marks the solution when non-evaporative flux (Q) is not considered (Q/P = 0, NSS), highlighting a local optimum with a higher objective function value. The yellow band indicates the expanded solution space and lower objective function values achieved when including Q, demonstrating the improved robustness and accuracy of ISONEVA in estimating E/P.

Moreover, ISONEVA avoids the common pitfalls associated with defining initial isotopic values associated with NSS. Many studies determine the initial isotopic composition using the intersection of the evaporation line (EL) with the local meteoric water line (LMWL) when using NSS framework (Benettin et al., 2021; Sprenger et al., 2017), implicitly assuming isotopic homogeneity and purely evaporative processes (Javaux et al., 2016). Heterogeneous mixing, new precipitation inputs, and vapor diffusion often disrupt these assumptions in soils. Importantly, the intersection-derived value does not necessarily represent the actual isotopic composition of the initial soil water storage (Benettin et al., 2018). Consequently, the EL-LMWL intersection often fails to reflect the true evaporation trajectory, potentially resulting in large initial value errors, up to -50‰ for δ^2H and -8‰ for $\delta^{18}O$ (Benettin et al., 2018). These errors can propagate through evaporation estimates, highlighting a critical limitation of NSS in natural, thus intrinsically heterogeneous, soil systems.

Additionally, the so-called "initial value" refers to the isotopic composition of water in the topsoil layer at a specific point in the solution of the governing partial differential equation (Gonfiantini, 1986). This "initial value" is relative rather than absolute: It does not necessarily correspond to the original isotopic compositions at the physical onset of evaporation. Instead, it marks the beginning of a defined calculation period.

ISONEVA circumvents this issue by redefining the initial value as a relative, temporally resolved parameter corresponding to the specific analysis period rather than an absolute physical starting point. This flexible treatment allows continuous, period-specific evaporation estimates without relying on potentially biased EL-LMWL intersections. Despite the increased computational complexity, ISONEVA offers a more reliable framework for estimating soil evaporation by improving the solution space and eliminating errors associated with initial value determination.

4.2 Practical considerations of ISONEVA for field applications

The practical application of ISONEVA requires measurements of topsoil water content and isotopic composition at the initial and final time points over a given evaluation period ($t_{initial}$ and t_{final}), together with basic meteorological data (e.g., air temperature and relative humidity). A key advantage is that it does not rely on direct, and often difficult, measurements of soil evaporation, transpiration, or percolation fluxes. ISONEVA is therefore particularly well suited for environments with intermittent rainfall, where precipitation events induce measurable changes in topsoil water storage and isotopic composition. By contrast, under extremely arid conditions without rainfall input ($P = 0$), ISONEVA cannot be applied to estimate E/P because the normalization by precipitation becomes undefined under such conditions.

Regarding temporal scale, ISONEVA performs best over sufficiently long evaluation intervals (e.g., monthly or longer), during which soil water storage and isotopic composition deviate meaningfully from their initial states. In other words, the time interval between $t_{initial}$ and t_{final} must be long enough to capture integrated soil-water and isotope dynamics. When this requirement is not met, substantial errors of approximated E/P ratios may occur (e.g., Figure 4a). By contrast, the SS method can be acceptable only under restrictive conditions: short time intervals and extremely thin surface layers (e.g., 0.01 m; Figure 5a) are difficult to achieve in routine field sampling and limit its broader applicability. Thus, ISONEVA represents a more robust option for estimating soil evaporation over monthly or longer timescales.

Virtual tests confirmed that ISONEVA achieves higher accuracy in E/P and Q/P estimation for a topsoil layer thickness of approximately 0.08 m when applied over long temporal intervals (> 30 days). In the field test, however, good performance is obtained even with a thicker topsoil layer (0.25 m) and a shorter evaluation period (< 20 days), which appears inconsistent with the virtual results. This discrepancy can be attributed to the use of isotope labelling experiments, which artificially enhanced the δ^2H and $\delta^{18}O$ gradients in the topsoil. The resulting signal amplification strengthened isotopic contrasts (Beyer

et al., 2020; Dubbert et al., 2022; Penna et al., 2018), improving the identifiability of evaporation and non-evaporative fluxes despite the thicker control volume.

We acknowledge that the optimal depth identified in the virtual experiment reflects the specific soil properties (light clay) and relatively frequent rainfall conditions considered in that setup. This optimal depth should therefore not be interpreted as universally applicable, particularly in extremely arid environments. Nevertheless, under typical field conditions, an effective depth near 0.08 m is fully consistent with the widely adopted practice of using the upper 0.05-0.1 m of soil to represent the evaporating layer, as this zone generally captures the dominant soil-water and isotopic dynamics relevant for evaporation. Broader cross-ecosystem generalization would require multi-site field datasets and represents an important direction for future research.

Overall, ISONEVA offers a valuable pathway for model evaluation and integration. It can be coupled with isotope-enabled land surface models to provide benchmark soil-water and isotope trajectories for evaluating model performance or to directly constrain model-estimated E/P ratios.

4.3 ISONEVA offers a robust and scalable diagnostic for soil evaporation

Partitioning ET into E and T remains a central challenge in ecohydrology, especially in arid and semi-arid ecosystems where E/T ratios fluctuate widely in space and time (Rothfuss et al., 2020; Williams et al., 2004). Accurate E estimation provides critical insights into soil–plant–atmosphere interactions, informing sustainable water management and improving understanding of subsurface water dynamics (Good et al., 2015; Sprenger et al., 2016).

Although ISONEVA-derived E/ET represents an upper bound, this conservative estimate is valuable for identifying whether evaporation dominates under specific conditions. By assuming that all transpiration occurs within the topsoil layer, the true E/ET value will always be lower than or equal to this upper bound. Thus, if measured E/ET exceeds this estimate, it suggests potential errors in model assumptions or flux measurements. This upper bound approach is also useful when transpiration is spatially variable or lacks direct measurements, providing a reliable reference point for hydrological assessments.

Compared to non-isotope-based ET partitioning methods, such as sap flow (Rafi et al., 2019), eddy covariance (EC) (Paul-Limoges et al., 2020), water-use-efficiency approaches (Yu et al., 2022), and evaporation-to-precipitation complementary methods (Wu et al., 2024; Zhang and Brutsaert, 2021), ISONEVA offers distinct advantages. Its strength lies in minimal data requirements, relying primarily on soil water content and isotopic composition, along with basic meteorological variables. This eliminates the need for detailed vegetation data (e.g., leaf area index, rooting depth) or the extensive calibration datasets often required by meteorological methods (Table 1; Stoy et al., 2019).

Table 1. Summary comparison of ISONEVA with other common ET partitioning approaches in terms of data requirements, ability to directly estimate soil evaporation, vegetation sensitivity, and scalability.

Approach	Data requirements	Soil E direct estimate	Vegetation sensitivity	Scalability
ISONEVA	Low to Moderate	Yes	Low	High
Sap flow	High	No	High	Low
WUE-based	Moderate to High	No	High	Moderate
Eddy covariance	High	No	Moderate	Moderate
E/P complementary	Moderate to High	No	Low	Variable

Moreover, as a soil-based approach, ISONEVA directly quantifies evaporation by constraining transpiration through soil water and isotope balances. This ensures its robustness, even under conditions of canopy-atmosphere decoupling or strong water stress. Consequently, ISONEVA shows lower sensitivity to transient physiological or atmospheric fluctuations than plant-centric methods coupled with photosynthesis.

Lastly, ISONEVA is inherently scalable. Its simple analytical framework and low data demands make it suitable for long-term, large-scale studies. This contrasts with plot-level sap flow or eddy covariance methods, which face logistical and cost limitations at larger scales. With advances in in-situ soil isotope monitoring (Beyer et al., 2020; Kühnhammer et al., 2022), regional to global applications of ISONEVA are becoming increasingly possible.

In summary, ISONEVA balances simplicity, robustness, and scalability, making it a powerful tool for soil evaporation and ET partitioning across diverse ecosystems and climates. These capabilities are critical for advancing our understanding of hydrological processes and informing agricultural and ecological water management strategies under changing climatic conditions.

5 Conclusions

This study introduces a novel isotope-based framework that explicitly incorporates non-evaporative fluxes to improve soil evaporation estimates. Traditional steady-state (SS) methods assume constant water and isotopic conditions, which are rarely met in natural soils, while non-steady-state (NSS) models neglect important non-evaporative processes such as infiltration and transpiration, leading to mass balance errors. By integrating both evaporative and non-evaporative fluxes, the proposed framework improves physical realism and enhances the accuracy and robustness of isotope-based estimates. Both virtual simulations and field tests demonstrate that this approach yields robust and realistic long-term estimates of evaporative and non-evaporative flux ratios relative to precipitation, outperforming traditional isotope-based methods. This enhanced capability provides valuable insights into water flux partitioning and plant water use strategies. Moreover, its minimal data requirements and consistent performance across scales make it especially suitable for regions where direct measurements are

scarce. These strengths position ISONEVA as a powerful tool for large-scale, long-term assessments of soil evaporation within the soil-plant-atmosphere continuum. Future research could further extend this framework by integrating remote sensing data or coupling it with hydrological models to improve regional and global evaporation estimates.

Appendix A. Derivations of NSS and ISONEVA

NSS

When express the water balance of the topsoil control volume under evaporation-only conditions, where the change in soil water storage ($\frac{\partial V}{\partial t}$) is equal to the evaporation flux E:

$$\frac{\partial V}{\partial t} = E \tag{A1}$$

Further, the isotopic mass balance can be written as:

$$\frac{\partial VR}{\partial t} = ER_E \tag{A2}$$

where VR is the total mass of isotopes in the control volume and ER_E is the isotopic flux associated with evaporation.

By applying the chain rule and combining Eq. A1, Eq. A2 can be rewritten as:

$$V\frac{\partial R}{\partial t} + R\frac{\partial V}{\partial t} = E(AR - B) \tag{A3}$$

$$V\frac{\partial R}{\partial t} = EAR - EB - ER \tag{A4}$$

Equation A4 describes the time evolution of soil isotopic composition as a function of the evaporation rate and the isotopic compositions of soil water and evaporated vapor.

Rewriting $v\frac{\partial R}{\partial t}$ in relation to $\frac{\partial (ln\, f)}{\partial t}$ yields:

$$V\frac{\partial R}{\partial t} = \frac{\partial R}{\partial (lnf)}\frac{\partial V}{\partial t} = -EB + (EA - E)R \tag{A5}$$

where f is the ratio of final to initial soil water storage.

Consequently, soil isotopic composition R can be written as a function of $ln\, f$, combining the water-storage change with isotopic enrichment processes:

$$\frac{\partial R}{\partial (lnf)} + (1 - A)R = -B \tag{A6}$$

Solving this first-order linear differential equation leads to Eq. A7, which provides the analytical solution for the evolution of R.

$$R = -\frac{B}{1-A} + f^{-(1-A)}\left(R_0 + \frac{B}{1-A}\right) \tag{A7}$$

Note that the partial differential equation like:

$$\frac{\partial y}{\partial x} + p(x)y(x) = q(x) \tag{A8}$$

has the analytical solution:

$$y = e^{-\int p(x)dx}\left(\int q(x)e^{\int p(x)\,dx}\,dx + constant\right) \tag{A9}$$

Equation A9 is used to derive Eq. A7 from Eq. A6 (also Eq. A17 from Eq. A16 below).

ISONEVA

Representing the water mass balance of the topsoil control volume, where changes in soil water storage ($\frac{\partial V}{\partial t}$) are determined by precipitation (P), evaporation (E), and percolation (Q):

$$\frac{\partial V}{\partial t} = P + E - Q \tag{A10}$$

Then, the isotopic mass balance can be written as:

$$\frac{\partial VR}{\partial t} = PR_P + ER_E - QR \tag{A11}$$

Equation A11 describes the corresponding isotope mass balance, where VR is the total mass of isotopes stored in the control volume. The terms on the right-hand side represent isotopic inputs from precipitation (PR_p), isotopic enrichment during evaporation (ER_E), and isotopic losses through percolation (QR).

To obtain an equation for the evolution of soil water isotopic composition (R), Eqs. A10 and A11 are combined and result in Eqs. A12-A14, which express the temporal evolution of R in terms of water fluxes and their isotopic compositions.

$$V\frac{\partial R}{\partial t} + R\,\frac{\partial V}{\partial t} = PR_P + E(AR - B) - QR \tag{A12}$$

$$V\frac{\partial R}{\partial t} = PR_P + EAR - EB - QR - PR - ER + QR \tag{A13}$$

$$V\frac{\partial R}{\partial t} = \frac{\partial R}{\partial (lnf)}\frac{\partial V}{\partial t} = PR_P - EB + (EA - P - E)R \tag{A14}$$

Like NSS derivations, Eq. A14 is rewritten in terms of the derivative of R with respect to $ln(f)$, this transformation yields Eq. A15.

$$\frac{\partial R}{\partial(lnf)}+\frac{(E+P-EA)}{P+E-Q}R=\frac{PR_P-EB}{P+E-Q} \tag{A15}$$

Finally, Eq. A15 can be further simplified to Eq. A16, which is a first-order linear differential equation. It can be solved analytically using Eq. A9 and results in Eq. A17, which is the basis of the ISONEVA estimation.

$$\frac{\partial R}{\partial(lnf)}+\frac{(1+x-Ax)}{1+x-y}R=\frac{R_P-Bx}{1+x-y} \tag{A16}$$

$$R=\frac{R_P-Bx}{1-Ax+x}+f^{\frac{1-Ax+x}{1+x-y}}\left(R_0-\frac{R_P-Bx}{1-Ax+x}\right) \tag{A17}$$

Appendix B. Sensitivity of SS, NSS, ISONEVA on atmospheric isotopic ratio

In the field validation of this study, we used the average atmospheric isotope values reported by Kurita et al. (2012) as the reference for estimating atmospheric vapor isotopes during evaporation. To enhance the reliability of the results, we employed field test data under a 23-day interval and used the upper and lower bounds of $\delta^{18}O$ (-27‰ to -13‰) and $\delta^{2}H$ (-199‰ to -94‰) measured by Kurita et al. (2012) to estimate E/P from the vegetated lysimeter. The results showed that soil evaporation estimates from the SS, NSS, and ISONEVA methods were insensitive to variations in atmospheric isotope values (Table S1), confirming the robustness of our field validation.

The limited sensitivity of SS, NSS, and ISONEVA to R_{atmos} (or δ_{atmos}) arises from the structure of the equation, where R_{atmos} only appears in the term B (Eqs. 16, 21, and 23). This term contributes additively and is divided by the kinetic fractionation factor, which dampens its overall influence. Additionally, when the residual water fraction f is close to 1 (i.e., limited evaporation), the output is dominated by the initial water isotope ratio R_0. Even under stronger evaporation conditions (low f), the exponential weighting still suppresses the impact of B, making the estimated E/P relatively insensitive to variations in atmospheric vapor isotopic composition.

Table B1. Estimated E/P ratios using the SS, NSS, and ISONEVA methods under different atmospheric isotopic compositions, based on field data measured by Nehemy et al. (2021) between June 6 and June 29. $\delta^{18}O_{atmos}$ and $\delta^{2}H_{atmos}$ are atmospheric isotopic compositions of oxygen-18 and deuterium, respectively.

	$\delta^{18}O_{atmos}$ = -27‰ $\delta^{2}H_{atmos}$ = -199‰	$\delta^{18}O_{atmos}$ = -20‰ $\delta^{2}H_{atmos}$ = -140‰	$\delta^{18}O_{atmos}$ = -13‰ $\delta^{2}H_{atmos}$ = -99‰
SS	-0.04	-0.04	-0.02
NSS	-0.01	-0.01	-0.005
ISONEVA	-0.1	-0.09	-0.12

Code and data availability

The codes are developed in MATLAB (https://doi.org/10.5281/zenodo.17119369) and distributed under the Creative Commons Attribution 4.0 International license. MOIST model is available from Fu & Si (2023) and the raw dataset of field measurements can be accessed from Nehemy et al. (2021).

Author contributions

Conceptualization: HF, BS, and WZ; Method development: HF and BS; Data collection, simulation, analyzation, and visualization: HF, MG, and HL; Writing and revision: HF, MG, HL, DP, JL, BS, and WZ.

Competing interests

None

Acknowledgments

This research was supported by the National Natural Science Foundation of China (42507413), National Key R & D Program of China (2022YFD1500100), Outstanding Youth Fund of Heilongjiang Province (JQ2024D002), China Agriculture Research System of MOF and MARA (CARS04).

References

Ads, A., Tziolas, N., Chrysikopoulos, C. V., Zhang, T. J., and Al Shehhi, M. R.: Quantitative analysis of water, heat, and salinity dynamics during bare soil evaporation, J Hydrol (Amst), 662, https://doi.org/10.1016/j.jhydrol.2025.133841, 2025.

Al-Oqaili, F., Good, S. P., Peters, R. T., Finkenbiner, C., and Sarwar, A.: Using stable water isotopes to assess the influence of irrigation structural configurations on evaporation losses in semiarid agricultural systems, Agric For Meteorol, 291, 108083, https://doi.org/10.1016/j.agrformet.2020.108083, 2020.

Bailey, A., Posmentier, E., and Feng, X.: Patterns of Evaporation and Precipitation Drive Global Isotopic Changes in Atmospheric Moisture, Geophys Res Lett, 45, 7093–7101, https://doi.org/10.1029/2018GL078254, 2018.

Benettin, P., Volkmann, T. H. M., Von Freyberg, J., Frentress, J., Penna, D., Dawson, T. E., and Kirchner, J. W.: Effects of climatic seasonality on the isotopic composition of evaporating soil waters, Hydrol Earth Syst Sci, 22, 2881–2890, https://doi.org/10.5194/hess-22-2881-2018, 2018.

Benettin, P., Nehemy, M. F., Asadollahi, M., Pratt, D., Bensimon, M., McDonnell, J. J., and Rinaldo, A.: Tracing and Closing the Water Balance in a Vegetated Lysimeter, Water Resour Res, 57, 1–18, https://doi.org/10.1029/2020WR029049, 2021.

Beyer, M., Kühnhammer, K., and Dubbert, M.: In situ measurements of soil and plant water isotopes: A review of approaches, practical considerations and a vision for the future, Hydrol Earth Syst Sci, 24, 4413–4440, https://doi.org/10.5194/hess-24-4413-2020, 2020.

Braud, I., Bariac, T., Gaudet, J. P., and Vauclin, M.: SiSPAT-Isotope, a coupled heat, water and stable isotope (HDO and H 218O) transport model for bare soil. Part I. Model description and first verifications, J Hydrol (Amst), 309, 277–300, https://doi.org/10.1016/j.jhydrol.2004.12.013, 2005.

Brooks, R. H. and Corey, A. T.: Hydraulic properties of porous media, Colorado State University, Fort Collins, 27 pp., 1964.

Dubbert, M., Cuntz, M., Piayda, A., Maguás, C., and Werner, C.: Partitioning evapotranspiration - Testing the Craig and Gordon model with field measurements of oxygen isotope ratios of evaporative fluxes, J Hydrol (Amst), 496, 142–153, https://doi.org/10.1016/j.jhydrol.2013.05.033, 2013.

Dubbert, M., Couvreur, V., Kubert, A., and Werner, C.: Plant water uptake modelling : added value of cross-disciplinary approaches, Plant Biol, https://doi.org/10.1111/plb.13478, 2022.

Fu, H. and Si, B.: MOIST Source code (Version 1.0) [Software], https://doi.org/10.5281/zenodo.8397416, 2023.

Fu, H., Neil, E. J., Li, H., and Si, B.: A Fully Coupled Numerical Solution of Water, Vapor, Heat, and Water Stable Isotope Transport in Soil, Water Resour Res, 61, https://doi.org/10.1029/2024WR037068, 2025.

Galewsky, J., Steen-Larsen, H. C., Field, R. D., Worden, J., Risi, C., and Schneider, M.: Stable isotopes in atmospheric water vapor and applications to the hydrologic cycle, Reviews of Geophysics, 54, 809–865, https://doi.org/10.1002/2015RG000512, 2016.

Gibson, J. J. and Reid, R.: Stable isotope fingerprint of open-water evaporation losses and effective drainage area fluctuations in a subarctic shield watershed, J Hydrol (Amst), 381, 142–150, https://doi.org/10.1016/j.jhydrol.2009.11.036, 2010.

Gonfiantini, R.: Handbook of environmental isotope geochemistry: The terrestrial environment, B Volume 2, vol. 18, edited by: Fritz, P. and Fontes, J. Ch., Elsevier, Armsterdam, 113–168, 1986.

Good, S. P., Noone, D., and Bowen, G.: Hydrologic connectivity constrains partitioning of global terrestrial water fluxes, Science (1979), 349, 175–177, https://doi.org/10.1126/science.aaa5931, 2015.

Haverd, V. and Cuntz, M.: Soil-Litter-Iso: A one-dimensional model for coupled transport of heat, water and stable isotopes in soil with a litter layer and root extraction, J Hydrol (Amst), 388, 438–455, https://doi.org/10.1016/j.jhydrol.2010.05.029, 2010.

Javaux, M., Rothfuss, Y., Vanderborght, J., Vereecken, H., and Bruggemann, N.: Isotopic composition of plant water sources, Nature, 525, 91–94, https://doi.org/10.1038/nature14983, 2016.

Kool, D., Agam, N., Lazarovitch, N., Heitman, J. L., Sauer, T. J., and Ben-Gal, A.: A review of approaches for evapotranspiration partitioning, Agric For Meteorol, 184, 56–70, https://doi.org/10.1016/J.AGRFORMET.2013.09.003, 2014.

Kurita, N., Newman, B. D., Araguas-Araguas, L. J., and Aggarwal, P.: Evaluation of continuous water vapor δd and δ18O measurements by off-axis integrated cavity output spectroscopy, Atmos Meas Tech, 5, 2069–2080, https://doi.org/10.5194/amt-5-2069-2012, 2012.

Mattei, A., Goblet, P., Barbecot, F., Guillon, S., Coquet, Y., and Wang, S.: Can soil hydraulic parameters be estimated from the stable isotope composition of pore water from a single soil profile?, Water (Switzerland), 12, https://doi.org/10.3390/w12020393, 2020.

Nehemy, M. F., Benettin, P., Asadollahi, M., Pratt, D., Rinaldo, A., and McDonnell, J. J.: Tree water deficit and dynamic source water partitioning, Hydrol Process, 35, https://doi.org/10.1002/hyp.14004, 2021.

Nelson, D. B., Basler, D., and Kahmen, A.: Precipitation isotope time series predictions from machine learning applied in Europe, Proc Natl Acad Sci U S A, 118, https://doi.org/10.1073/pnas.2024107118, 2021.

Nicholls, E. M. and Carey, S. K.: Evapotranspiration and energy partitioning across a forest-shrub vegetation gradient in a subarctic, alpine catchment, J Hydrol (Amst), 602, https://doi.org/10.1016/j.jhydrol.2021.126790, 2021.

Nicholls, E. M., Clark, M. G., and Carey, S. K.: Transpiration and evaporative partitioning at a boreal forest and shrub taiga site in a subarctic alpine catchment, Yukon territory, Canada, in: Hydrological Processes, https://doi.org/10.1002/hyp.14900, 2023.

Or, D., Lehmann, P., Shahraeeni, E., and Shokri, N.: Advances in Soil Evaporation Physics-A Review, Vadose Zone Journal, 12, vzj2012.0163, https://doi.org/10.2136/vzj2012.0163, 2013.

Paul-Limoges, E., Wolf, S., Schneider, F. D., Longo, M., Moorcroft, P., Gharun, M., and Damm, A.: Partitioning evapotranspiration with concurrent eddy covariance measurements in a mixed forest, Agric For Meteorol, 280, https://doi.org/10.1016/j.agrformet.2019.107786, 2020.

Penna, D., Hopp, L., Scandellari, F., Allen, S. T., Benettin, P., Beyer, M., Geris, J., Klaus, J., Marshall, J. D., Schwendenmann, L., Volkmann, T. H. M., Von Freyberg, J., Amin, A., Ceperley, N., Engel, M., Frentress, J., Giambastiani,

Y., McDonnell, J. J., Zuecco, G., Llorens, P., Siegwolf, R. T. W., Dawson, T. E., and Kirchner, J. W.: Ideas and perspectives: Tracing terrestrial ecosystem water fluxes using hydrogen and oxygen stable isotopes - Challenges and opportunities from an interdisciplinary perspective, Biogeosciences, 15, 6399–6415, https://doi.org/10.5194/BG-15-6399-2018, 2018.

Rafi, Z., Merlin, O., Le Dantec, V., Khabba, S., Mordelet, P., Er-Raki, S., Amazirh, A., Olivera-Guerra, L., Ait Hssaine, B., Simonneaux, V., Ezzahar, J., and Ferrer, F.: Partitioning evapotranspiration of a drip-irrigated wheat crop: Inter-comparing eddy covariance-, sap flow-, lysimeter- and FAO-based methods, Agric For Meteorol, 265, 310–326, https://doi.org/10.1016/j.agrformet.2018.11.031, 2019.

Rothfuss, Y., Quade, M., Brüggemann, N., Graf, A., Vereecken, H., and Dubbert, M.: Reviews and syntheses: Gaining insights into evapotranspiration partitioning with novel isotopic monitoring methods, Biogeosciences Discussions, 1–48, https://doi.org/10.5194/bg-2020-414, 2020.

Shokri, N., Lehmann, P., Vontobel, P., and Or, D.: Drying front and water content dynamics during evaporation from sand delineated by neutron radiography, Water Resour Res, 44, 1–11, https://doi.org/10.1029/2007WR006385, 2008.

Sprenger, M., Leistert, H., Gimbel, K., and Weiler, M.: Illuminating hydrological processes at the soil-vegetation-atmosphere interface with water stable isotopes, https://doi.org/10.1002/2015RG000515, 1 September 2016.

Sprenger, M., Tetzlaff, D., and Soulsby, C.: Soil water stable isotopes reveal evaporation dynamics at the soil-plant-atmosphere interface of the critical zone, Hydrol Earth Syst Sci, 21, 3839–3856, https://doi.org/10.5194/hess-21-3839-2017, 2017.

Stoy, P. C., El-Madany, T. S., Fisher, J. B., Gentine, P., Gerken, T., Good, S. P., Klosterhalfen, A., Liu, S., Miralles, D. G., Perez-Priego, O., Rigden, A. J., Skaggs, T. H., Wohlfahrt, G., Anderson, R. G., Coenders-Gerrits, A. M. J., Jung, M., Maes, W. H., Mammarella, I., Mauder, M., Migliavacca, M., Nelson, J. A., Poyatos, R., Reichstein, M., Scott, R. L., and Wolf, S.: Reviews and syntheses: Turning the challenges of partitioning ecosystem evaporation and transpiration into opportunities, Biogeosciences, 16, 3747–3775, https://doi.org/10.5194/bg-16-3747-2019, 2019.

Trenberth, K. E., Fasullo, J. T., and Kiehl, J.: Earth's Global Energy Budget, Bull Am Meteorol Soc, 90, 311–324, https://doi.org/10.1175/2008BAMS2634.1, 2009.

Vereecken, H., Schnepf, A., Hopmans, J. W., Javaux, M., Or, D., Roose, T., Vanderborght, J., Young, M. H., Amelung, W., Aitkenhead, M., Allison, S. D., Assouline, S., Baveye, P., Berli, M., Brüggemann, N., Finke, P., Flury, M., Gaiser, T., Govers, G., Ghezzehei, T., Hallett, P., Hendricks Franssen, H. J., Heppell, J., Horn, R., Huisman, J. A., Jacques, D., Jonard, F., Kollet, S., Lafolie, F., Lamorski, K., Leitner, D., McBratney, A., Minasny, B., Montzka, C., Nowak, W., Pachepsky, Y., Padarian, J., Romano, N., Roth, K., Rothfuss, Y., Rowe, E. C., Schwen, A., Šimůnek, J., Tiktak, A., Van Dam, J., van der

Zee, S. E. A. T. M., Vogel, H. J., Vrugt, J. A., Wöhling, T., and Young, I. M.: Modeling soil processes: review, key challenges, and new perspectives, Vadose Zone Journal, 15, 1539–1663, https://doi.org/10.2136/vzj2015.09.0131, 2016.

Volkmann, T. H. M. and Weiler, M.: Continual in situ monitoring of pore water stable isotopes in the subsurface, Hydrol Earth Syst Sci, 18, 1819–1833, https://doi.org/10.5194/hess-18-1819-2014, 2014.

Williams, D. G., Cable, W., Hultine, K., Hoedjes, J. C. B., Yepez, E. A., Simonneaux, V., Er-Raki, S., Boulet, G., De Bruin, H. A. R., Chehbouni, A., Hartogensis, O. K., and Timouk, F.: Evapotranspiration components determined by stable isotope, sap flow and eddy covariance techniques, Agric For Meteorol, 125, 241–258, https://doi.org/10.1016/j.agrformet.2004.04.008, 2004.

Wu, Q., Yang, J., Song, J., and Xing, L.: Improvement in the blending the evaporation precipitation ratio with complementary principle function for daily evaporation estimation, J Hydrol (Amst), 635, https://doi.org/10.1016/j.jhydrol.2024.131170, 2024.

Xiang, W., Si, B., Li, M., Li, H., Lu, Y., Zhao, M., and Feng, H.: Stable isotopes of deep soil water retain long-term evaporation loss on China's loess plateau, Science of The Total Environment, 147153, https://doi.org/10.1016/j.scitotenv.2021.147153, 2021.

Yidana, S. M., Fynn, O. F., Adomako, D., Chegbeleh, L. P., and Nude, P. M.: Estimation of evapotranspiration losses in the vadose zone using stable isotopes and chloride mass balance method, Environ Earth Sci, 75, 1–18, https://doi.org/10.1007/s12665-015-4982-6, 2016.

Yu, L., Zhou, S., Zhao, X., Gao, X., Jiang, K., Zhang, B., Cheng, L., Song, X., and Siddique, K. H. M.: Evapotranspiration Partitioning Based on Leaf and Ecosystem Water Use Efficiency, Water Resour Res, 58, https://doi.org/10.1029/2021WR030629, 2022.

Zhang, L. and Brutsaert, W.: Blending the Evaporation Precipitation Ratio With the Complementary Principle Function for the Prediction of Evaporation, Water Resour Res, 57, https://doi.org/10.1029/2021WR029729, 2021.

Zhou, T., Šimůnek, J., and Braud, I.: Adapting HYDRUS-1D to simulate the transport of soil water isotopes with evaporation fractionation, Environmental Modelling and Software, 143, https://doi.org/10.1016/j.envsoft.2021.105118, 2021.